polymers

MDPI

Supporting Information

The role of chain molecular weight and Hofmeister series ions in thermal aggregation of poly(2-isopropyl-2-oxazoline) grafted nanoparticles

Martina Schroffenegger[1], Ronald Zirbs[1], Steffen Kurzhals[1] and Erik Reimhult[1,*]

[1] University of Natural Resources and Life Sciences Vienna, Muthgasse 11, 1190 Vienna, Austria; martina.schroffenegger@boku.ac.at (M.S.); ronald.zirbs@boku.ac.at (R.Z.); steffen.kurzhals@boku.ac.at (S.K.)

* Correspondence: erik.reimhult@boku.ac.at; Tel.: +43 1 47654-80211

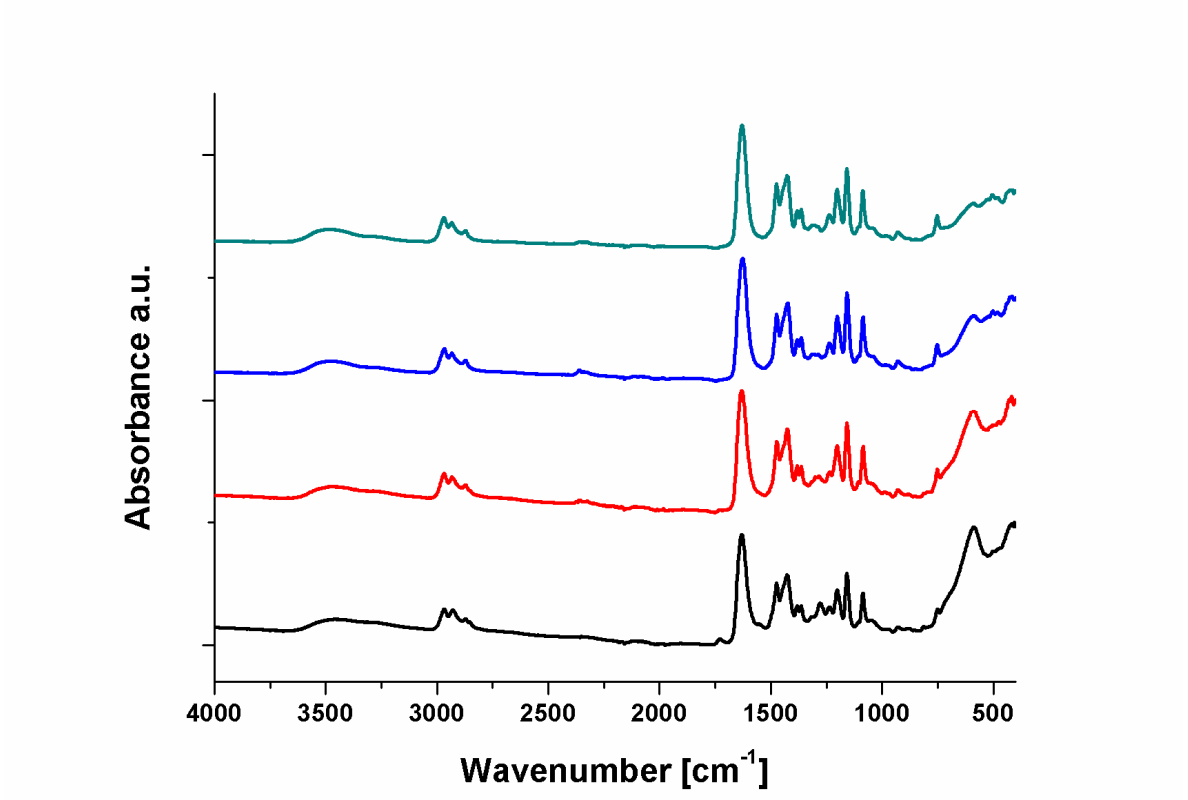

Figure S1. FTIR spectra of SPION samples. Black: FeOx-6, red: FeOx-14, blue: FeOx-21 and cyan: FeOx-33.

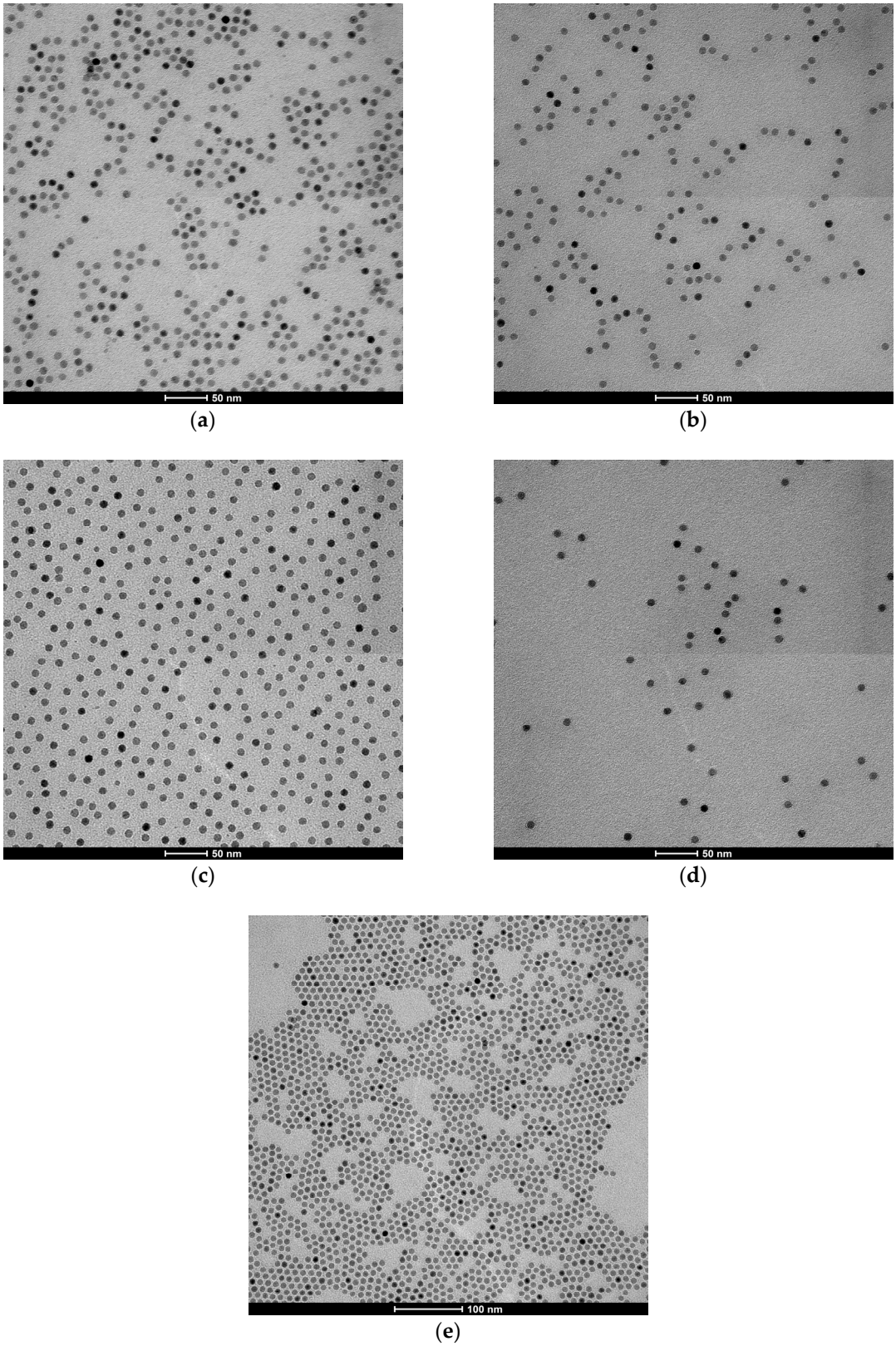

Figure S2. Transmission electron micrographs of 9.1 nm diameter SPION grafted with PiPOx of different MW, **(a)**: FeOx-6 (grafted with PiPOx 6 kg mol^{-1}), **(b)**: FeOx-14 (grafted with PiPOx 14 kg mol^{-1}), **(c)**: FeOx-21 (grafted with PiPOx 21 kg mol^{-1}) and **(d)**: FeOx-33 (grafted with PiPOx 33 kg mol^{-1}), (**e**) oleic acid coated SPION.

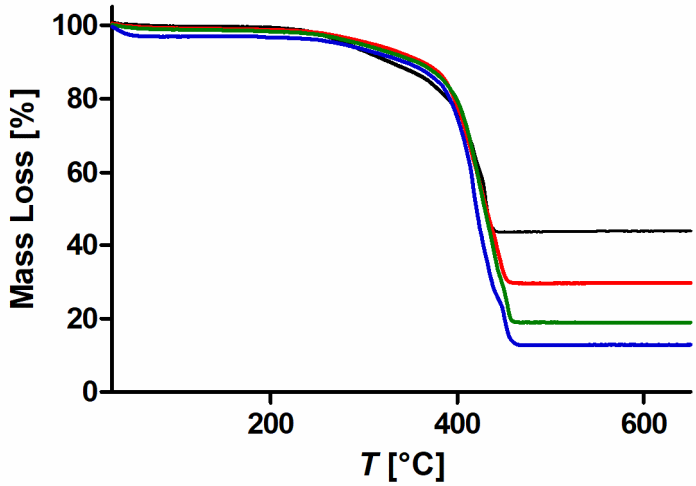

Figure S3. TGA curves of all SPION samples. TGA was measured with a heating rate of 10 °C min^{-1} at a constant flow of 80 mL min^{-1} of synthetic air. Black: FeOx-6, red: FeOx-14, green: FeOx-21, blue: FeOx-33.

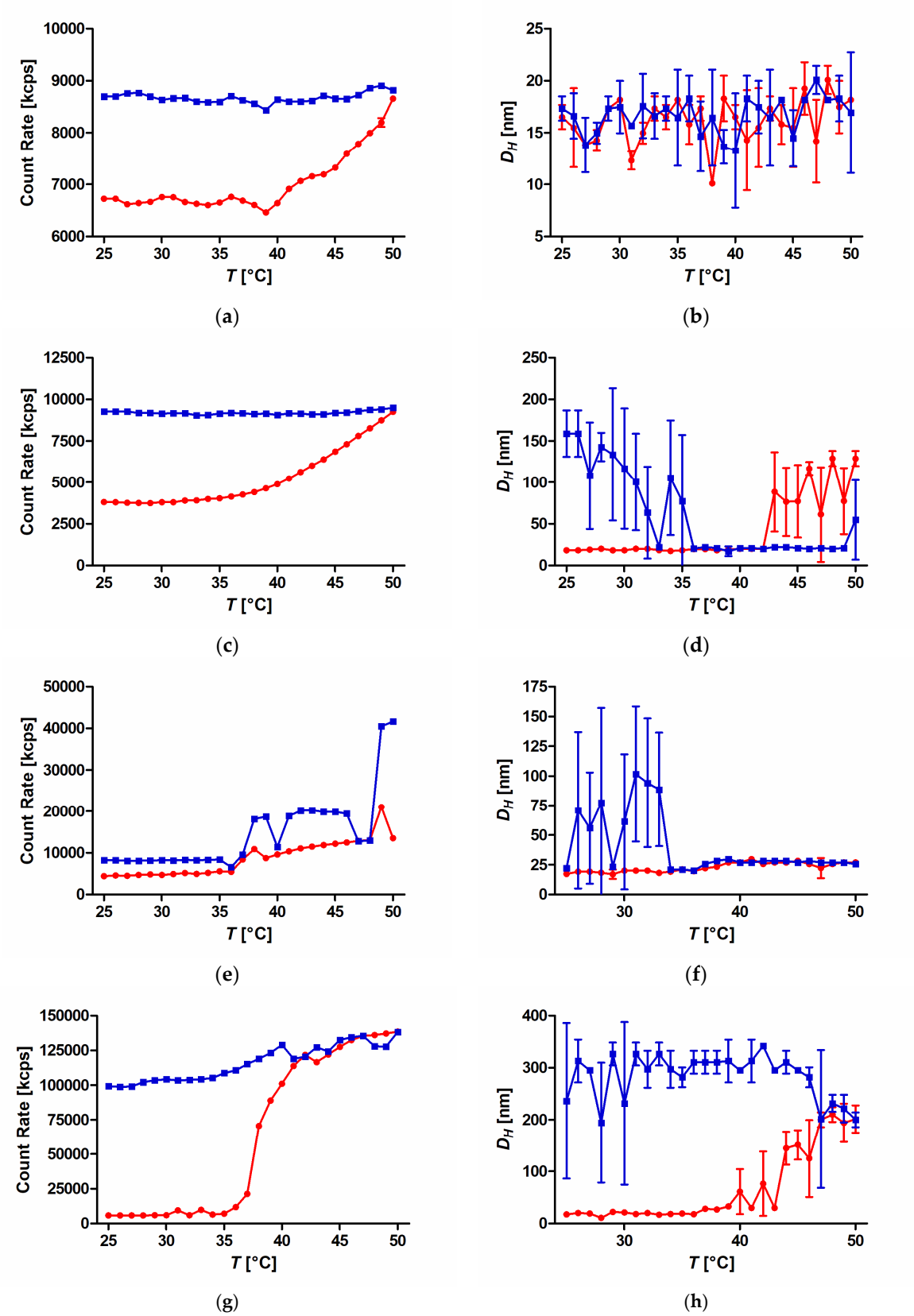

Figure S4. Temperature-cycled DLS of PiPOx grafted SPION dispersions measured at a concentration of $5 \cdot 10^{13}$ particles per mL: FeOx-6: (**a**) and (**b**), FeOx-14: (**c**) and (**d**), FeOx-21: (**e**) and (**f**), FeOx-33: (**g**) and (**h**). Left: count rate *vs* temperature, right: hydrodynamic diameter (D_H) *vs* temperature. In red circles: heating curve, in blue squares: cooling curve. Mean values and standard deviation of count rate and number weighted diameter were calculated from three measurements for each temperature step.

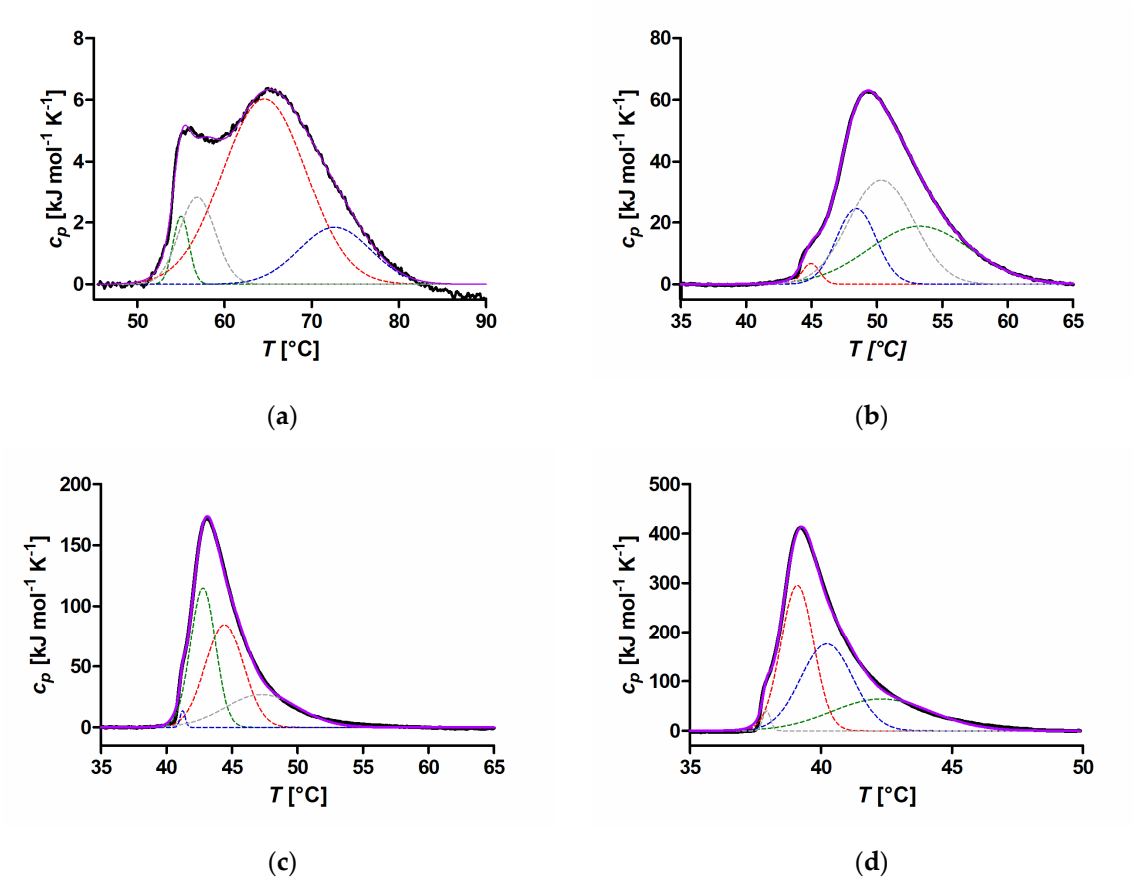

Figure S5. DSC curves of free polymer PiPOx samples. The samples were measured with a concentration of 1 g L^{-1} in Milli-Q water with a heating rate of 60 °C h^{-1}. (**a**): PiPOx-6, (**b**): PiPOx-14, (**c**): PiPOx-21 and (**d**): PiPOx-33. Black: raw data of the measurements, dashed lines: fitted curves, violet: sum of fitted curves.

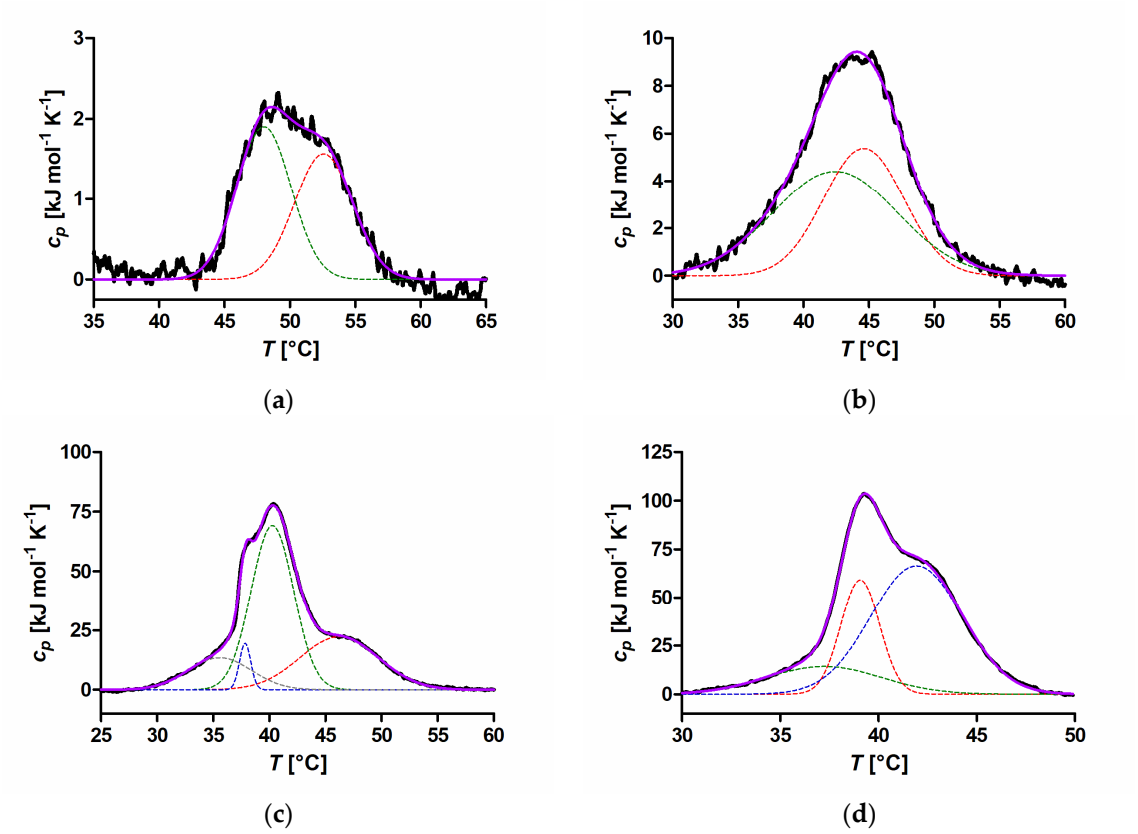

Figure S6. DSC curves of core-shell iron oxide nanoparticles. The samples were measured with a concentration of 1 g L^{-1} in Milli-Q water with a heating rate of 60 °C h^{-1}. (**a**): FeOx-6, (**b**): FeOx-14, (**c**): FeOx-21 and (**d**): FeOx-33. Black: raw data of the measurements, dashed lines: fitted curves, violet: sum of fitted curves.

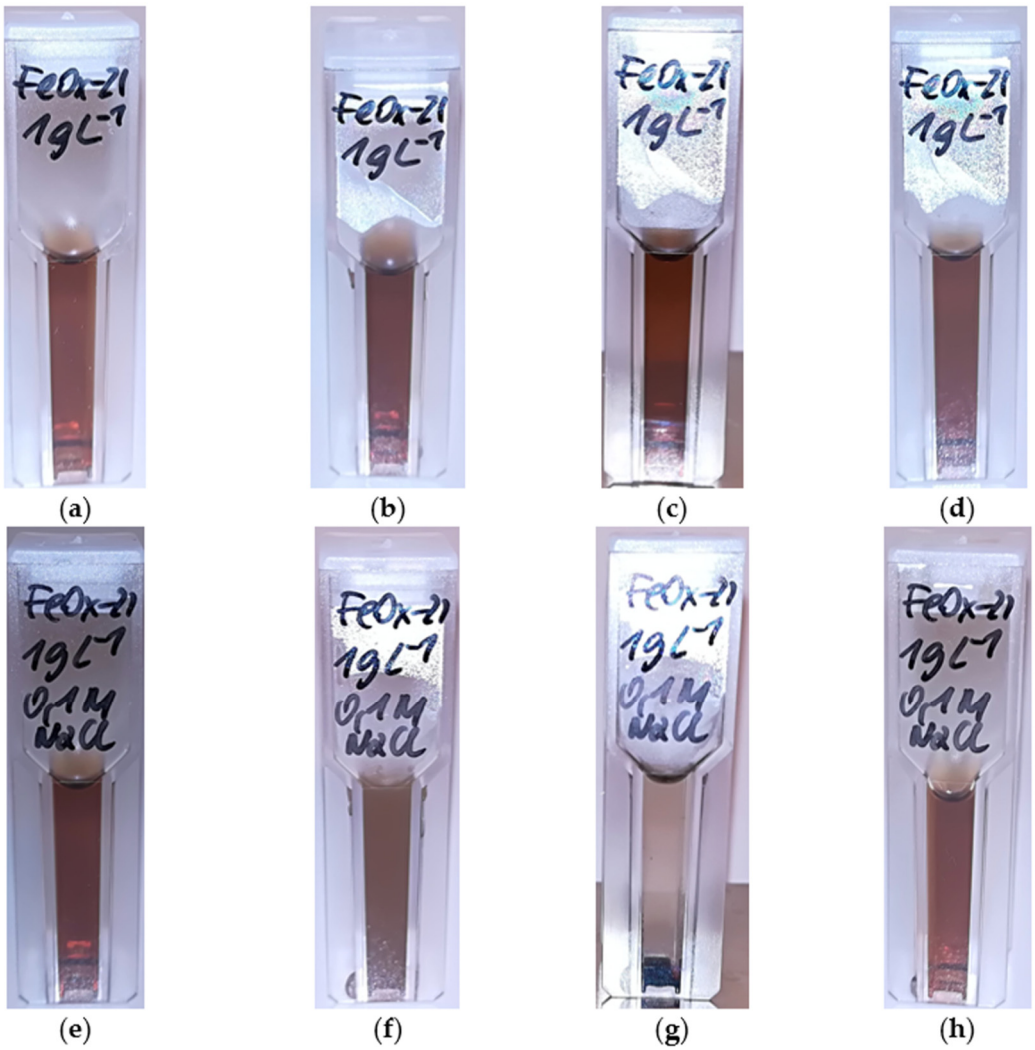

Figure S7. Photographs of colloidal stability of core-shell SPION FeOx-21 dispersions at a concentration of 1 g L^{-1} in Milli-Q water. Upper row, without salt, lower row with a NaCl concentration of 0.1 M. (**a**) and (**e**) at room temperature, (**b**) and (**f**) at 50 °C, (**c**) and (**g**) at 50 °C on a static magnet (remanence = 1.29 T), (**d**) and (**h**) after cooling to room temperature.

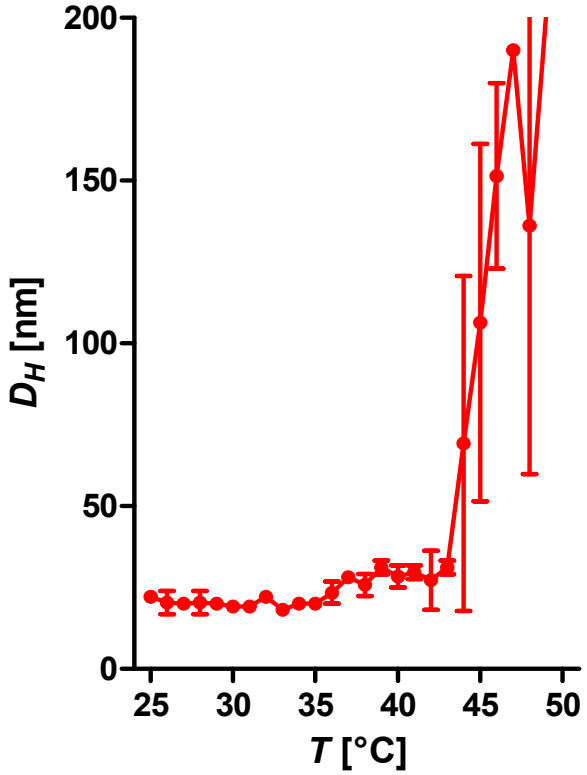

Figure S8: Temperature-cycled DLS for FeOx-33 dispersions in Milli-Q at a concentration of 1g L^{-1}: hydrodynamic diameter (D_H) *vs* temperature of the heating curve is enlarged.

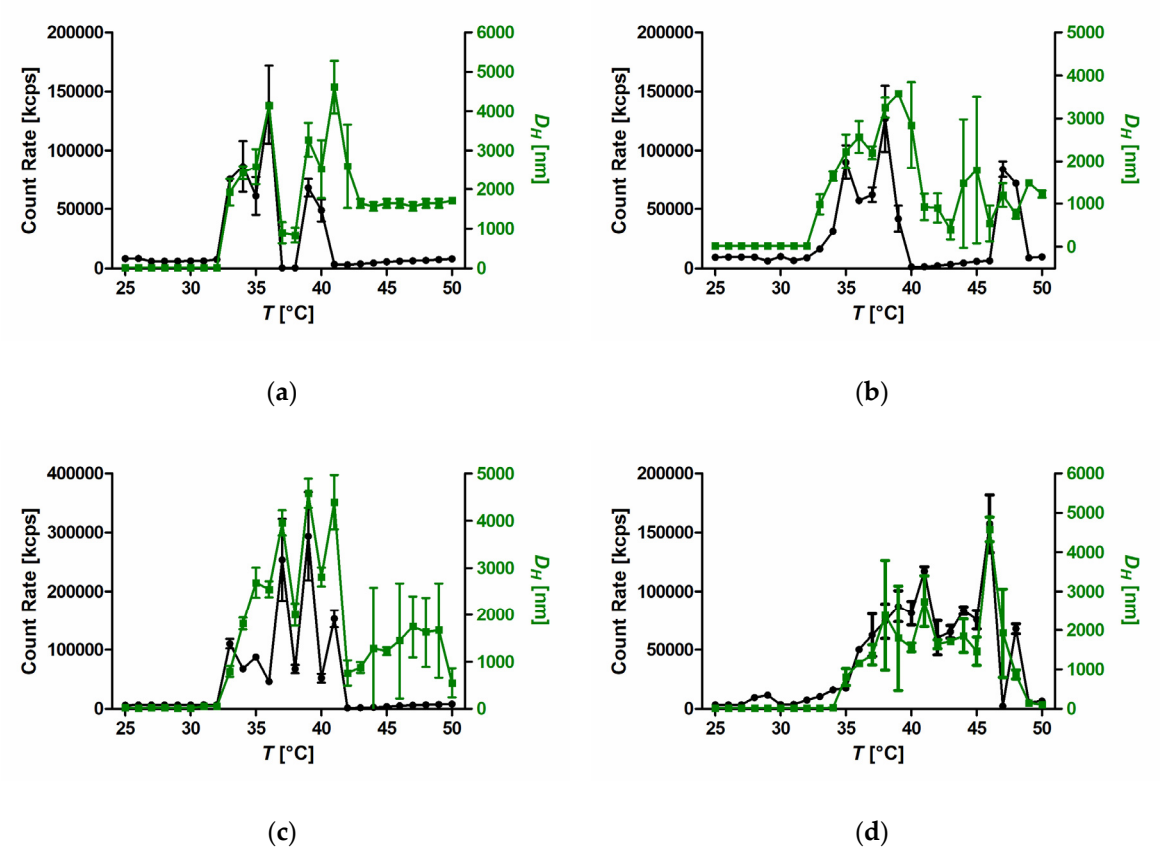

Figure S9. DLS-heating curves for core-shell SPION (FeOx-21, 1g L^{-1}) dispersions with different concentrations of $CaCl_2$. (**a**): 0.01 M $CaCl_2$, (**b**): 0.05 M $CaCl_2$, (**c**): 0.1 M $CaCl_2$, (**d**): 0.16 M $CaCl_2$. Black: count rate and in green hydrodynamic diameter curve. Mean values and standard deviation of count rate and number weighted diameter were calculated from three measurements for each temperature step.

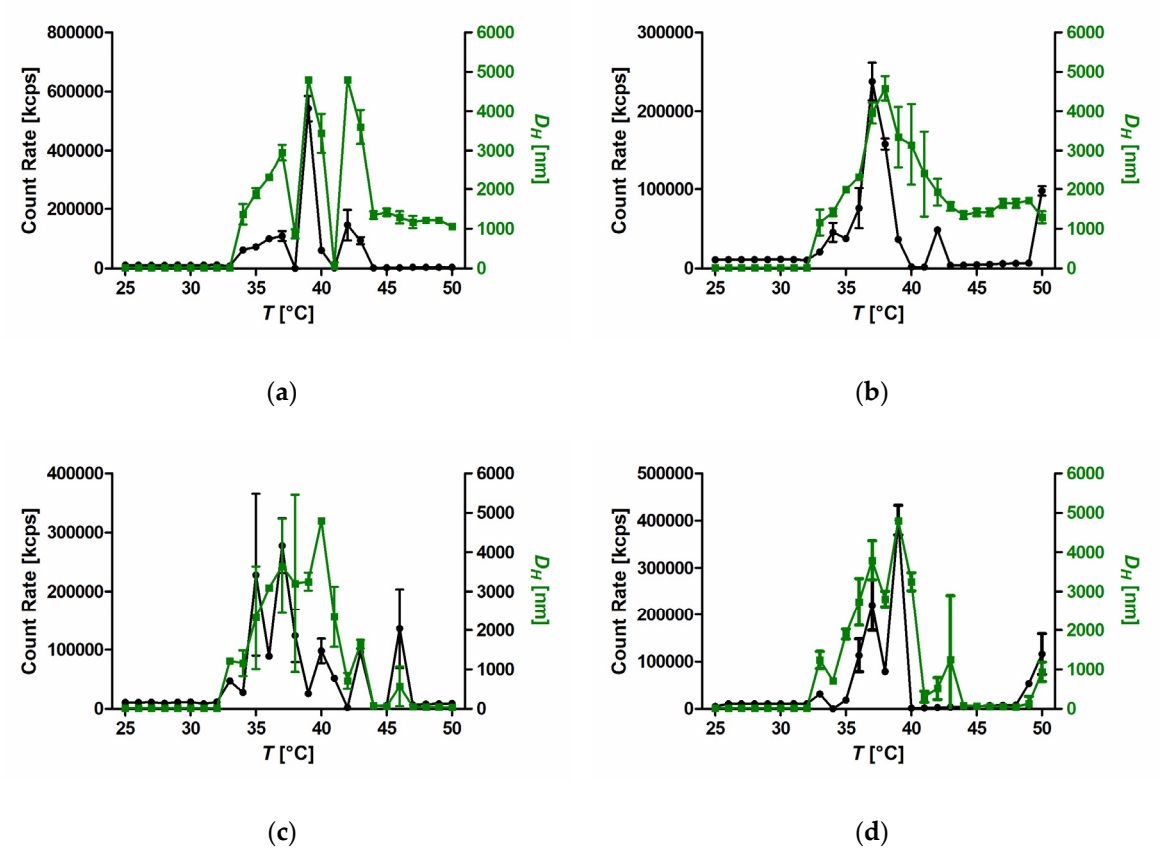

Figure S10. DLS-heating curves for core-shell SPION dispersions (FeOx-21, 1g L^{-1}) with different concentrations of KCl. (**a**): 0.01 M KCl, (**b**): 0.05 M KCl, (**c**): 0.1 M KCl, (**d**): 0.16 M KCl. Black: count rate and in green hydrodynamic diameter curve. Mean values and standard deviation of count rate and number weighted diameter were calculated from three measurements for each temperature step.

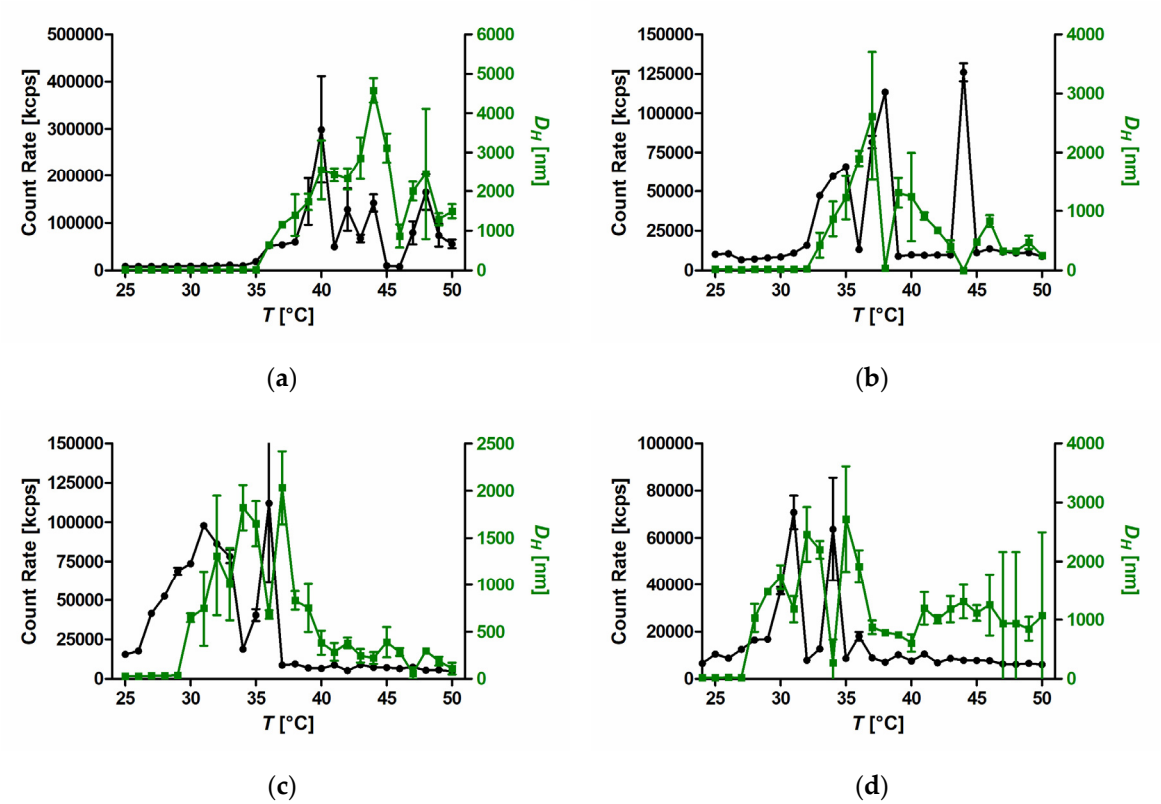

Figure S11. DLS-heating curves for core-shell SPION dispersions (FeOx-21, 1g L^{-1}) with different concentrations of NaH_2PO_4. (**a**): 0.01 M NaH_2PO_4, (**b**): 0.05 M NaH_2PO_4, (**c**): 0.1 M NaH_2PO_4, (**d**): 0.16 M NaH_2PO_4. Black: count rate and in green hydrodynamic diameter curve. Mean values and standard deviation of count rate and number weighted diameter were calculated from three measurements for each temperature step.

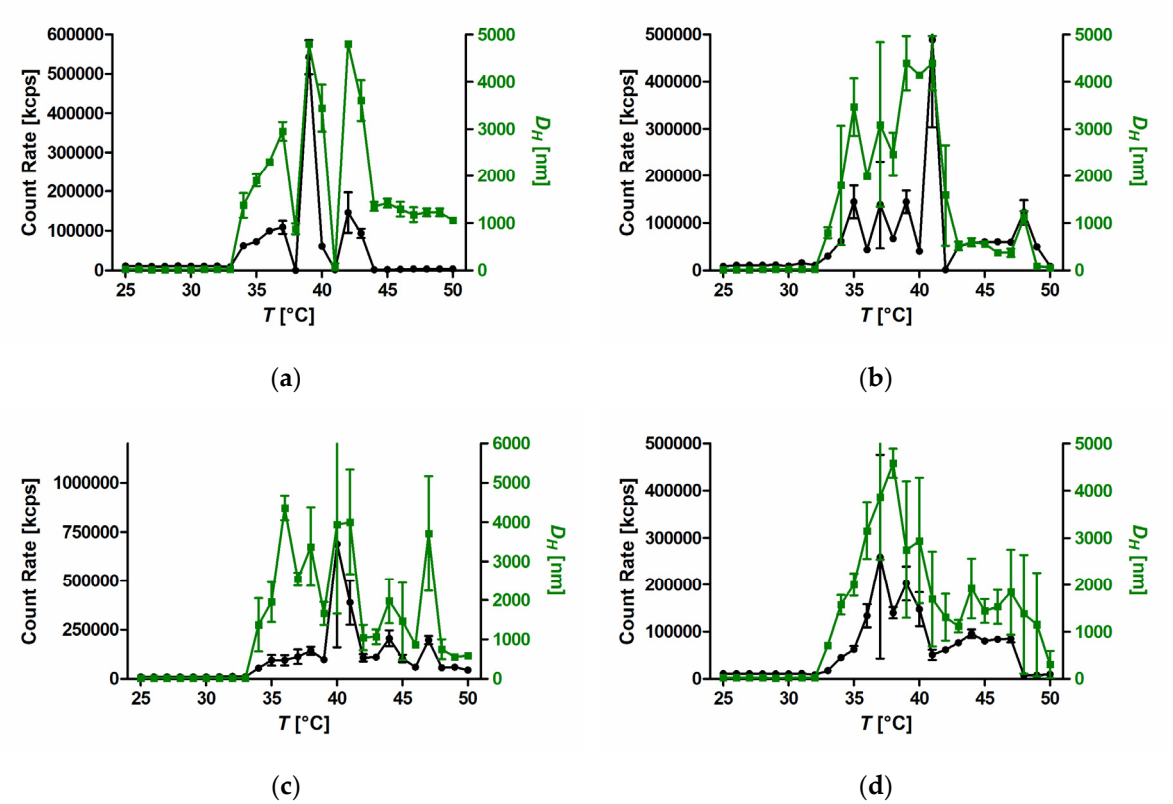

Figure S12. DLS-heating curves for core-shell SPION dispersions (FeOx-21, 1g L^{-1}) with different concentrations of $MgCl_2$. (**a**): 0.01 M $MgCl_2$, (**b**): 0.05 M $MgCl_2$, (**c**): 0.1 M $MgCl_2$, (**d**): 0.16 M $MgCl_2$. Black: count rate and in green hydrodynamic diameter curve. Mean values and standard deviation of count rate and number weighted diameter were calculated from three measurements for each temperature step.

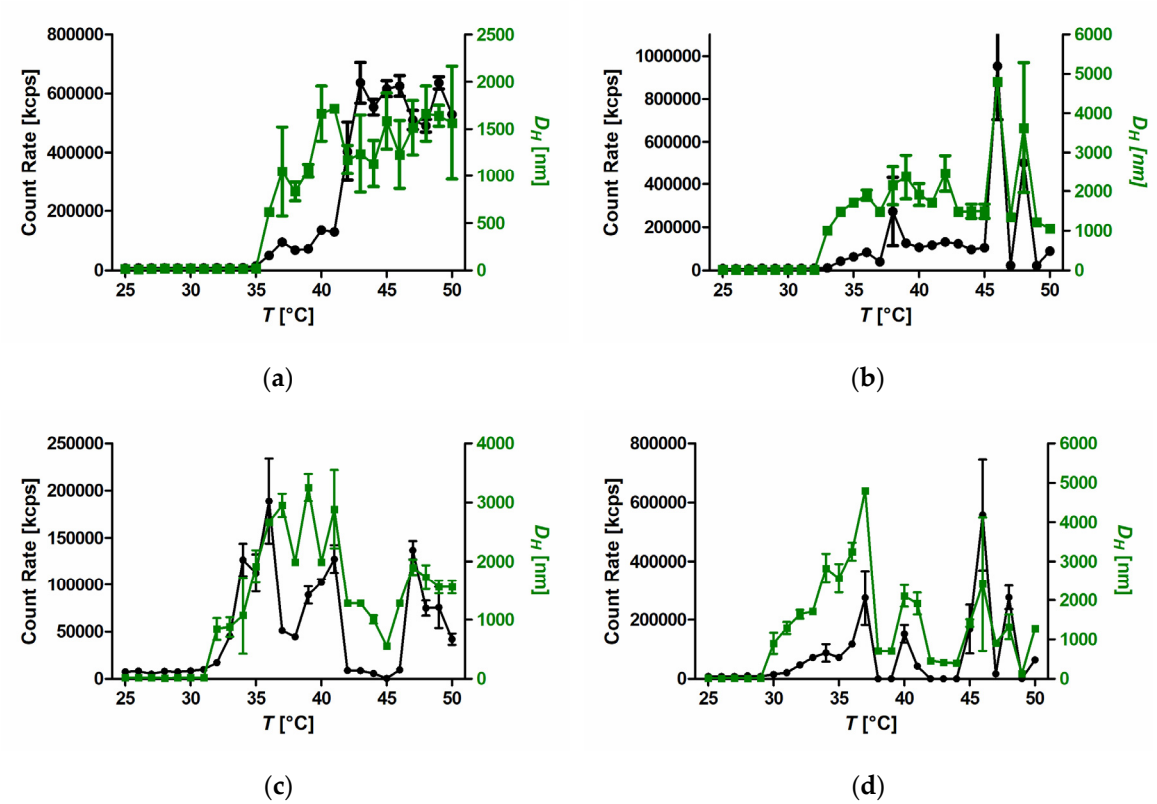

Figure S13. DLS-heating curves for core-shell SPION dispersions (FeOx-21, 1g L^{-1}) with different concentrations of $NaHCO_3$. (**a**): 0.01 M $NaHCO_3$, (**b**): 0.05 M $NaHCO_3$, (**c**): 0.1 M $NaHCO_3$, d: 0.16 M $NaHCO_3$. Black: count rate and in green hydrodynamic diameter curve. Mean values and standard deviation of count rate and number weighted diameter were calculated from three measurements for each temperature step.